SPE 115678

Modeling Particle Gel Propagation in Porous Media

Yu-Shu Wu, SPE, Colorado School of Mines, and Baojun Bai, SPE, Missouri University of Science and Technology

Abstract

Gel treatments are a proven cost-effective method to reduce excess water production and improve sweep efficiency in waterflood reservoirs. A newer trend in gel treatments uses particle gel (PG) to overcome some distinct drawbacks inherent in *in-situ* gelation systems. In this paper, we present a conceptual numerical model, based on laboratory tests and analyses, to simulate PG propagation through porous rock. In particular, we use a continuum modeling approach to simulate PG movement and its impact on isothermal oil and water flow and displacement processes. In this conceptual model, the PG is treated as one additional "component" to the water phase. This simplified treatment is based on the following physical considerations: (1) PG is mobilized only within the aqueous phase by advection in reservoirs; (2) PG, once retained in the porous media, will occupy pore space in pore bodies or pore throats and therefore reduce the permeability to bypassing water or oil; and (3) PG mobilization may not occur through pores or pore throats until some thresholds in pressure and/or pressure gradients are achieved and these threshold conditions are described by analogy to non-Newtonian fluid or non-Darcy flow in porous media, i.e., by a modified Darcy's law. The model is able to predict and evaluate the effects of PG as a conformance control agent to improve oil production and control excess water production.

Introduction

Excess water production has become a major problem for oilfield operators to deal with, as more and more reservoirs, subject to long-term water flooding, become mature. In addition to rapid reduction in oil recovery, high rates of water production also create many problems from corrosion and fluid-handling facility to waste water handling and eventually lead to well shut-in. Consequently, many producing zones are often abandoned in an attempt to avoid water contact, even when the formations still contain large volumes of remaining hydrocarbons. Controlling water production has become more and more important to both the oil industry and environmental protection.

Gel treatments, if used properly, are very effective to improve reservoir conformance and to reduce excess water production during oil and gas production. Traditionally *in-situ* gels have been widely used for these purposes. The mixture of polymer and crosslinker, called gelant, is injected into target formation and reacts to form gel to fully or partially seal the formation at reservoir temperature (Sydansk, 1992; Jain, 2005). Thus the gelation occurs in reservoir conditions. A new trend in gel treatments is applying preformed gels, because the preformed gels are formed at surface facilities before injection, no gelation occurs in reservoirs, so they can overcome some distinct drawbacks inherent in *in-situ* gelation systems, such as lack of gelation time control, uncertainness of gelling due to shear degradation, chromatographic fractionation or change of gelant compositions, and dilution by formation water. The preformed gels include preformed bulk gels (Seright, 2004), partially preformed gels (Sydansk, 2004 and 2005), and particle gels which include mm-sized preformed particle gel (PPG) (Li, 1999; Coste 2000; Bai, 2004 and 2007), microgels (Chauveteau, 2001 and 2003; Rousseau 2005; Zaitoun 2007) and pH sensitive crosslinked polymer (Al-Anazi, 2002; Huh, 2005), mm-sized swelling polymer grains which is a similar product with PPG (Pyziak et al., 2007; Larkin and Creel, 2008; Abbasy et al., 2008), and Bright Water® (Pritchett, 2003; Frampton, 2004). Their major differences are in their sizes and swelling times. Published documents indicate that several particle gels were economically applied to reduce water production in mature oilfields. Microgel was applied to one gas storage well to reduce water production (Zaitoun, 2007). Bright water was used for more than 10 wells treatments with BP and Chevron (Cheung, 2007). PPGs were applied in about 2,000 wells to reduce fluid channels in waterfloods and polymer floods in China (Liu, 2006; Bai, 2008). Recently, Occidental Oil Company (Pyziak et al., 2007) and Kinder-Morgan (Larkin and Creel, 2008) used the mm-sized swelling polymer grains to control CO_2 breakthrough for their CO_2 flooding areas and promising results have been found.

To understand particle gel transport through porous media, Bai et al. (2007) reported their experimental results of PPG

propagation through porous media and observed the particle behavior in porous media through visual micromodels. Abbasy et al. (2008) reported the experimental results on the plugging efficiency of mm-sized swelling polymer grains on fractures. However, no mathematical model has been reported and few quantitative studies have been carried out to model the elastic particle gel propagation through porous media. In this paper, we present a conceptual mathematical model, based on our laboratory tests and analyses, to simulate PG flow through porous rock and to predict how particle gel to mobile and impact oil and water flow from reservoirs to wells.

Experiment
Experimental studies on behavior and characteristics of particle gel transport through porous media in this section as well as the previous work data (Bai, 2001 and 2007) provide our basis for building a mathematical model to simulate gel particle propagation through porous media.

Flow Patterns: In our previous work (Bai et al. 2007), core-flooding tests were performed on sandpack cores to understand the particle gel propagation through porous media. Three types of flow patterns were identified: *pass, broken and pass*, and *plug*. The characterization and typical flow curves for each pattern are discussed as follows.

Pass: Figure 1 shows a typical pressure change over time for the *pass* pattern. In this example, 1,000 mg/L soft particle suspensions with an average particle size of 250 mesh were injected into a sandpack core, prepared using 20 mesh quartz sands. The injection pressure did not obviously increase at the first 4 PV suspension injection. Effluent analysis showed no particle produced at the outlet during this period, indicating the particles were retained within the porous media. After 4 PV of suspension injection, the injection pressure started to increase near linearly. When the volume of the injected particle suspensions reached to certain amount (about 6.2 PV in this case), the pressure was stabilized to around 0.012 MPa with little change, and a plateau appeared. The pressure in the middle (point B) of the core showed the same trends. It is clear that a stable particle suspension flow of through the core can be reached. The effluent particle size and concentration are the same as injected, as shown in Fig. 2 and Table 1. In addition, the resistance factor (Fr) during the particle injection and the residual resistance factor (Frr) during water injection after particle injection are almost the same for different segment along the core, as shown in Table 2.
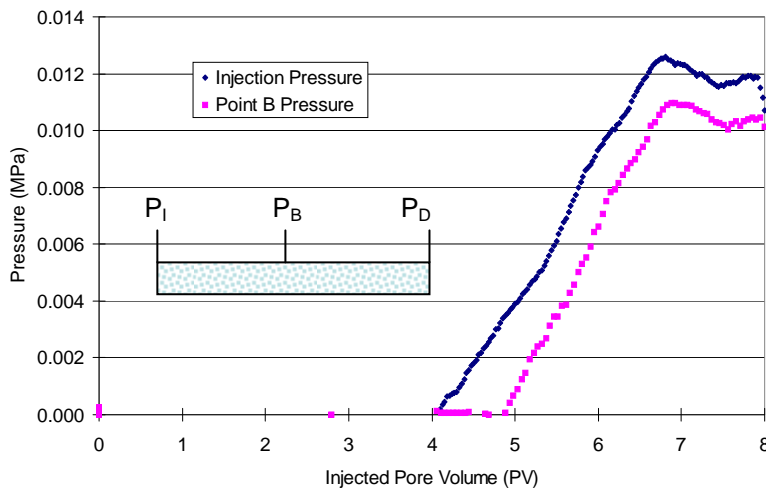

Fig.1   A typical pressure curve for the "*pass*" pattern.

(a) particles before

(b) particles from effluent

Fig.2   Particle size comparison

Table 1. Resistance Factor and Residual Resistance Factor Data for "*pass*" pattern.

1, 000 mg/L PPG injection				Water Injection after PPG injection	
Stable injection pressure	Resistance factor			Residual Resistance Factor	
	IB	BD		IB	BD
0.0125	7.1	6.4		6.40	6.32

Note: I is the injection point located in the core inlet, and B is in the middle of the core and D is the core outlet open to the atmosphere.

Broken and Pass: the pressure variation trend is the same as the "*pass*" pattern, as shown as Fig.3. For this example, 250-mesh soft particle suspension was injected into the core, prepared using 40 mesh sands. Compared with the injected particle shown in Fig. 2(a), the effluent size pf particles shown Figure 3 was significantly reduced, different from "*pass*" pattern. Table 2 also shows the significant change of the average particle size from 0.236 mm before particle injection to

0.139 mm after transporting through the core. Table 3 presents the resistance factor Fr and residual resistance factor Frr along the core. The Fr and Frr in the first segment was higher than those in the second segment, and the Fr and Frr are still much greater than those in Table 1, which indicates that some particles moved into this segment and flow resistance was built up.
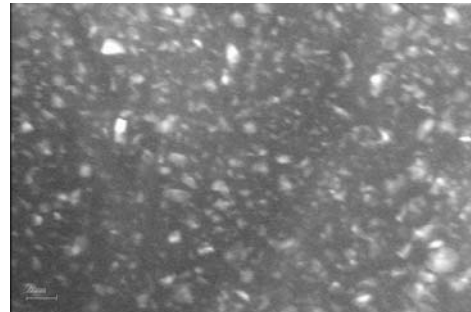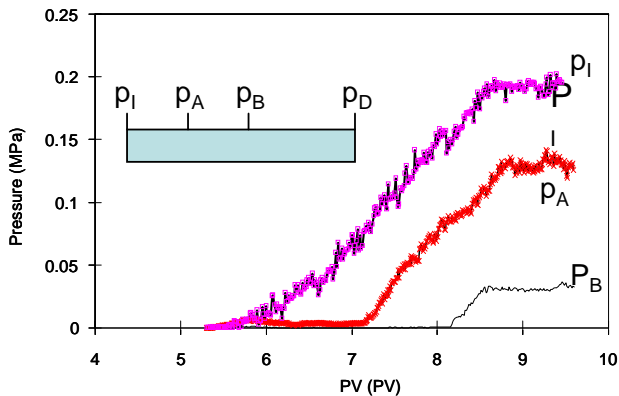

Fig.3   A typical pressure change for the "*broken and pass*" pattern. (note: the A point is in the middle of I and B)

Fig.4   Particle image from effluent

Table 2. The particle size change before and after pass through core

Particle	Average particle size（mm）	Standard Variance	Average roundness
Before injection	0.236	0.158	1.64
After injection	0.139	0.073	3.3

Table 3. Resistance factor and residual resistance factor data for "*broken and pass*" Pattern.

1000 mg/L PPG injection				Water Injection after PPG injection	
Stable injection pressure（MPa）	Resistance factor			Residual Resistance Factor	
	IB	BD		IB	BD
0.19	50.5	21.6		31.3	12.3

Plug: The injection pressure rapidly increases until it reaches the maximum pressure that the apparatus can deal with, but the pressure in the middle tap does not change. Figure 4 gives a typical curve for the case. In this case, 160 mesh soft particle suspensions with a concentration of 1,000 mg/L were injected 24 Darcy core, prepared using 60 mesh sands (the ratio of swollen particle size to throat is 8.8). The pressure rapidly increased to 1 MPa when 1.2 PV particle suspension was injected. Water injection was resumed for about 2.8 PV and the water injection pressure went down. After that, the particle suspension was injected again and the pressure increased much faster than that during the first injection. The pressure rapidly increased to 3.2 MPa, the maximum pressure that the apparatus can resist, with 1.2 PV particle suspension injection. However, the pressure in the middle did not change at all. At this time, no particle was produced from the outlet of the core. The Fr and Frr in the first segment are usually quite large, but they remain at one in the second segment, and the results are shown in Table 4.
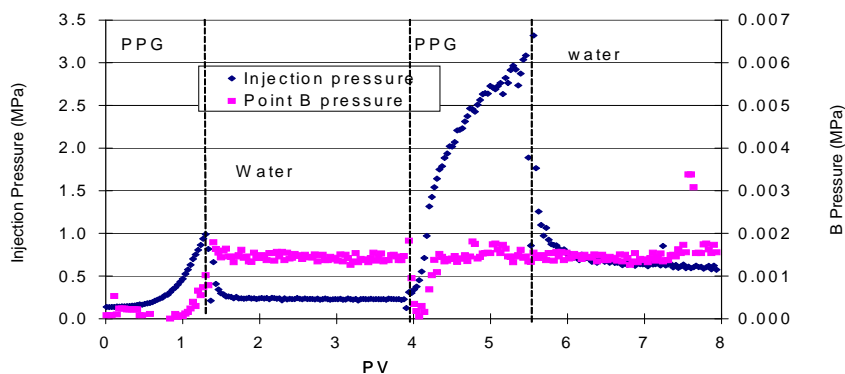

Fig. 4. A typical curve for the "*Plug*" pattern.

Table 4. Resistance factor and residual resistance factor for "*plug*" pattern.

1,000 mg/L PPG injection				Water Injection after PPG injection	
Stable injection pressure	Resistance factor			Residual Resistance Factor	
	IB	BD		IB	BD
No	599	1.0		105	1.0

Note: the maximum injection pressure that the apparatus can take is at 3 MPa.

Threshold Pressure Gradient for Elastic Particle Flow: Swollen gel particles are different from other traditional particles in that the gel particles are deformable, and they can pass through the pore throats smaller than particles themselves by deformation (Bai et al., 2007). However, the particle movement requires a threshold pressure gradient, i.e., the minimum pressure gradient to force the particles to move through a porous medium. The threshold pressure gradient depends mainly on the ratio of particle diameters to average pore size. Table 5 shows the relationship between them, which was taken from the figure in the previous publication (Bai, 2007). As shown in Table 5, the threshold pressure gradient is relatively small for weak (or soft) gel, when the ratio is smaller than 2.9. Also, but its value shows little change when the ratio increases from 3.7 to 6.6. For hard particles, however, the threshold pressure gradient change significantly from 0.083 to 0.67 MPa/m when the ratio of particle diameters to average pore size increases from 2 to 2.5 only.

Table 5. Relationship of threshold pressure gradient and ratio of particle diameters and pore size

Soft Particle			Hard Particle	
Ratio of particle to pore throat	threshold pressure Gradient (MPa/m)		Ratio of particle to pore throat	threshold pressure gradient (MPa/m)
2.9	0.04		2	0.083
3.7	0.7		2.5	0.67
3.9	0.7			
6.6	0.8			

Particle Retention in Porous Media: <u>Particle Gel:</u> Two kinds of PPG particles, the same as the previous publication (Bai, 2007), were used for the experiment – hard particle and soft particle. The first swollen gel with swollen capacity of 70, called "soft particle," is much more deformable than the second one, which has a swollen capacity of 30, called "hard particle".

   <u>**Core Flooding Tests:**</u> A steel tube with a length of 26 cm and an inner diameter of 1.9 cm was used for all core-flooding tests. The tube was packed 20~40 mesh of quartz sands with permeability of around 65 D and a porosity of 45%. Four concentrations of hard and soft particles were injected into a core until effluent particle concentration was equal to injected particle concentration. Effluent samples were collected from the outlet to analyze particle concentration. The particles are not completely carried by with water flow and part of them will retain in the porous media due to gravitation deposition, adsorption or interaction with pore surfaces. The difference between accumulative injected particles and produced particles is the retained particle mass, which can be used to calculated retention density by dividing by the sand mass in the tube. Figure 6 showed the two particles retention density as the function of original particle concentrations. The retention density increases with the injected particle concentration for either kind of particles themselves. The hard particles have a higher retention than the soft ones because they are harder to move through pore or pore throats.
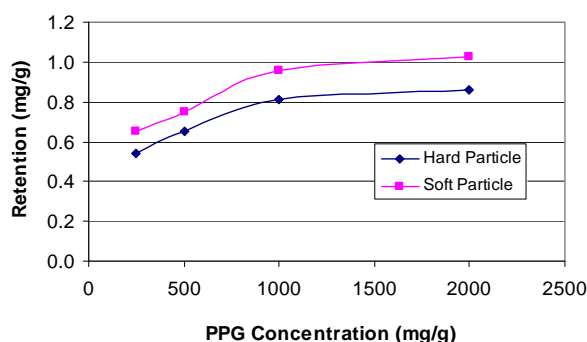

Fig.6.   Particle gel retention on the core with a permeability of 65 D.

Conceptual and Mathematical Model

We propose use the continuum modeling approach to simulate particle gel movement within the aqueous phase in isothermal oil and water two-phase flow systems. In this conceptual model, the particle gel is treated to be a "solute", i.e., as an additional "component" to the water phase. This simplified assumption or treatment is based on the experimental results discussed in the section above and the following physical considerations:

- Particle gel is mobilized only in the aqueous phase by advection with three types of flow patterns: *pass, broken and pass*, and *plug,* and subject to retention within porous rock;

- Particle gel, once entering and existing in porous media, will take pore space and may be retarded in pore bodies or throats and therefore reduce effective permeability to fluid flow;
- Particle gel mobilization may not occur through pores or pore throats until some thresholds in pressure and/or pressure gradients are reached *in situ* and these threshold conditions may be described by analogy with non-Newtonian (and/or non-Darcy) fluid flow in porous media, i.e., by a modified Darcy's law.

According to mass conservation principles for a two-phase, isothermal system consisting of three components: water, oil, and PG, a generalized conservation equation of the three mass components in the porous continuum can be written as follows:

$$\frac{\partial M^k}{\partial t} = G^k + q^k + F^k \tag{1}$$

where superscript k is the index for the components; k = w for water, o for oil, and p for PG; M is the mass accumulation term of component k; G^k (k=p) is the decay or dissolution (or degradation) term of PG; q^k is an external source/sink term or fracture-matrix exchange term for mass component k; and F^k is the "flow" term of mass movement or net exchange from multiphase flow or advective mass transport.

The accumulation terms in (1) for the component oil is evaluated as

$$M^o = \phi \rho_o S_o \tag{2}$$

where ϕ is the porosity of porous media; ρ_o is density of oil phase; and S_o is saturation of oil phase.

Note that the aqueous phase consists of two mass components water and PG. If we assume no mass exchange among oil, water phases and PG, in our conceptual model, we may handle PG as a "phase," which may actually be not continous. Therefore, in the model formulation, phases are exchangeable with mass components. We have

$$M^w = \phi \rho_w S_w \tag{3}$$

and

$$M^p = \phi \rho_p S_p + (1-\phi)\rho_s \rho_p S_p K_d^p \tag{4}$$

In Equations (3) and (4), ρ_w and ρ_p are densities, respectively, of water and PG in their respective phase; S_w and S_p are saturations, respectively, of water phase and PG in porous media; and K_d^p is the distribution coefficient of component PG between the aqueous phase and rock solids to account for particle adsorption or retention effects. The decay or dissolution term of PG may be expressed as:

$$G^p = \phi \lambda_p \left(\phi \rho_p S_p + (1-\phi)\rho_s \rho_p S_p K_d^p \right) \tag{5}$$

where λ_p is the first-order decay or degradation constant of component PG to account for PG degradation effects. From their definition of saturations, it turns out

$$S_o + S_w + S_p = 1 \tag{6}$$

To evaluate F^k, the "flow" term in (1), the Darcy's law is assumed to be valid for both aqueous (water+PG) and oil multiphase flow with accompany of PG with the following modification (Wu et al., 1992),

$$\mathbf{v}_\beta = -\frac{k^* k_{r\beta}}{\mu_\beta}\left(\nabla \Phi_\beta^e\right) \qquad (\beta=\text{o and a}) \tag{7}$$

where P_β and μ_β are pressure and viscosity of fluid phase β [=o oil and =a for aqueous phase (including water and PG)], respectively; $k_{r\beta}$ is the relative permeability to phase β; and k^* is a modified absolute or intrinsic permeability, is treated as a function of PG saturation (i.e., PG concentration); and the effective flow potential gradient is defined as,

$$\nabla \Phi_\beta^e = \left(\nabla \Phi_\beta - G_\beta\right) \quad \text{if } \nabla \Phi \geq G_\beta \tag{8a}$$

$$\nabla \Phi_\beta^e = \left(\nabla \Phi_\beta + G_\beta\right) \quad \text{if } \nabla \Phi \leq -G_\beta \tag{8b}$$

$$\nabla \Phi_\beta^e = 0 \qquad\qquad \text{if } \left|\nabla \Phi\right| \leq G_\beta \tag{8c}$$

The potential gradient is defined as,

$$\nabla \Phi_\beta = \nabla P_\beta - \rho_\beta g \nabla z \tag{9}$$

where g is gravitational constant; z is the vertical coordinate; and the aqueous phase density is defined as,

$$\rho_a = \rho_w S_w + \rho_p S_p \tag{10}$$

The mass flow terms in (1) are then determined as:

$$F^o = \nabla \cdot (\rho_o \mathbf{v}_o) \tag{11}$$

$$F^w = \nabla \cdot (S_w \rho_w \mathbf{v}_a) \tag{12}$$

and

$$F^p = \nabla \cdot (S_p \rho_p \mathbf{v}_a) \tag{13}$$

Once the terms and parameters in (7) are known, simulation of oil-water two-phase flow with PG transport becomes a black-oil modeling problem by using (7) in (11), (12), and (13) for oil, water, and PG flow terms. These flow terms are then substituted into mass balance Equation (1).

Constitutive Relationships: To complete the mathematical description of multiphase flow with PG propagation, Equation (1), a generalized mass-balance equation, needs to be supplemented with a number of constitutive equations. These constitutive correlations express interrelationships and constraints of physical processes, variables, and parameters, and allow the evaluation of secondary variables and parameters as functions of a set of primary unknowns or variables selected to make the governing equations solvable. Table 6 lists a commonly used set of constitutive relationships used in describing multiphase flow and particle transport through porous and fractured media in this work. Many of these correlations for estimating properties and interrelationships are determined by experimental studies.

To simulate PG prorogation through porous or fractured rock, we introduce four new correlations:

(1)   The PG distribution coefficient K_d^p, in (4), for adsorption or retention onto rock solids and should be experimental determined, as shown in Figure 6, as a function of PG concentration, C_p, in the aqueous phase:

$$K_d^p = K_d^p (C_p) \tag{13}$$

where C_p, particle concentration, is estimated by,

$$C_p = \frac{S_p \rho_p}{S_p + S_w} \tag{14}$$

(2)   The PG decay or dissolution coefficient, λ_p, is the first-order decay constant to account for PG *in-situ* degradation effects in (5).

(3)   The particle-gel modified permeability may be written as:

$$k^* = \frac{k}{Fr(C_p)} \tag{15}$$

where k is intrinsic permeability, Fr is flow resistance factor and treated as a function of aqueous PG concentration.

(4)   The phase threshold pressure gradient may be written as:

$$G_\beta = G_\beta (C_p, k) \tag{16}$$

a function of aqueous PG concentration and intrinsic permeability, and the latter dependence is used to account for pore size, which has a significant impact on flow resistance and threshold pressure gradient.

The actual functional forms of Fr and G_p should be determined using lab experiments and field data.

Table 6. Constitutive Relationships and Functional Dependence

Definition	Function	Description
Fluid saturation	$S_o + S_a = 1$	Constraint on summation of total fluid saturations.
Capillary pressure	$P_o = P_w + P_{C\beta} (S_\beta)$	In a multiphase system, the capillary pressure relates pressures between the oil and aqueous phases and is defined as a function of fluid saturation.
Relative permeability	$k_{r\beta} = k_{r\beta} (S_\beta)$	The relative permeability of a fluid phase in oil and aqueous phase systems is assumed to be functions of fluid saturation.
Fluid density	$\rho_\beta = \rho_\beta (P)$	Density of fluid phases and PG is treated as a function of pressure only (β=o, a and p).
Fluid viscosity	$\mu_\beta = \mu_\beta (P)$	Functional dependence or empirical expressions of viscosity of oil and aqueous fluids is treated as a function of pressure.
Porosity	$\phi = \phi (P)$	Porosity is treated as a function of pressure.

Numerical Formulation

The methodology for numerical approaches to simulate multiphase subsurface flow and PG transport consists of the following three steps: (1) spatial discretization of mass conservation equations, (2) time discretization; and (3) iterative approaches to solve the resulting nonlinear, discrete algebraic equations. Among various numerical techniques for simulation studies, a mass--conserving discretization scheme, based on finite or integral finite-difference or control-volume finite-element methods, is the most commonly used approach, and is discussed here.

Discrete Equations: The three mass- balance equations [Equation (1)] are discretized in space using an integral finite-difference method (Fig. 1) (Pruess et al., 1999). Time discretization is carried out using a backward, first-order, fully implicit finite-difference scheme. The discrete nonlinear equations for components of water, and oil, and PG at gridblock or node i can be written in a general form:

$$\left\{ M_i^{k,n+1} + G_i^{k,n+1}\Delta t - M_i^{k,n} \right\}\frac{V_i}{\Delta t} = \sum_{j\in\eta_i} flow_{ij}^{k,n+1} + Q_i^{k,n+1} \tag{17}$$

(k = 1, 2, and 3 for oil, water and particle gel) and (i=1, 2, 3, …, N)

where superscript k serves as an equation index for all mass conservation equations with k = 1, 2, and 3 denoting the oil, water and PG; superscript n denotes the previous time level, with n+1 the current time level to be solved; subscript i refers to the index of gridblock or node i, with N being the total number of nodes in the grid; Δt is time step size; V_i is the volume of node i; η_i contains the set of direct neighboring nodes (j) of node i; M_i^k, G_i^k, $flow_{ij}^k$, and Q_i^k are the accumulation and degradation/generation terms for PG (k=3) only, respectively, at node i; the "flow" term between nodes i and j, and sink/source term at node i for component k, respectively, are defined below. Equation (17) has the same form regardless of the dimensionality of the system, i.e., it applies to one-, two-, or three-dimensional flow and transport analyses. The accumulation and decay/generation terms for the three mass components are evaluated using Equations (2) to (5), respectively, at each node i. The "flow" terms in Equation (17) are generic and for mass fluxes by advective processes, as described by Equations (11), (12), and (13), i.e., the mass flux of fluid phase β and PG transport along the connection is given, respectively, by

$$flow_{ij}^o = \lambda_{o,ij+1/2}\rho_{o,ij+1/2}\gamma_{ij}\left(\Delta\Phi_{oji}^e\right) \qquad \text{for oil} \tag{18a}$$

$$flow_{ij}^w = \lambda_{a,ij+1/2}\left(\rho_w S_w\right)_{ij+1/2}\gamma_{ij}\left(\Delta\Phi_{aji}^e\right) \qquad \text{for water} \tag{18b}$$

$$flow_{ij}^p = \lambda_{a,ij+1/2}\left(\rho_p S_p\right)_{ij+1/2}\gamma_{ij}\left(\Delta\Phi_{aji}^e\right) \qquad \text{for PG} \tag{18c}$$

where $\lambda_{\beta,ij+1/2}$ is the mobility term to oil and aqueous phase β (= o and a), defined as

$$\lambda_{\beta,ij+1/2} = \left(\frac{k_{r\beta}}{\mu_\beta}\right)_{ij+1/2} \tag{19}$$

In Equation (18), γ_{ij} is transmissivity and is defined differently for finite-difference or finite-element discretization. If the integral finite-difference scheme (Pruess et al. 1999) is used, the transmissivity is evaluated as

$$\gamma_{ij} = \frac{A_{ij}k_{ij+1/2}^*}{D_i + D_j} \tag{20}$$

where A_{ij} is the common interface area between connected blocks or nodes i and j (Fig. 7); and D_i is the distance from the center of block i to the interface between blocks i and j (Fig. 7).
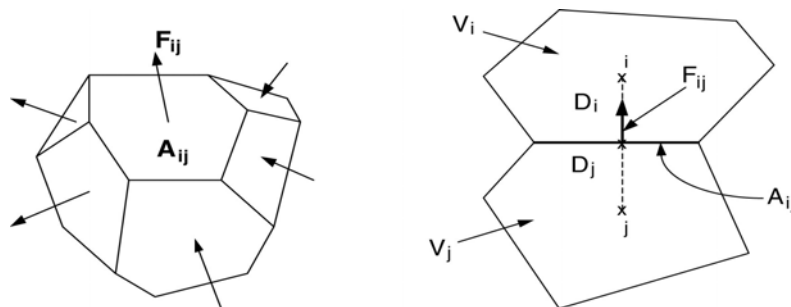

Fig. 7.   Space discretization and flow-term evaluation in the integral finite difference method (Pruess, 1991)

In evaluating the "flow" terms in the above Equations (18) - (20), subscript ij+1/2 is used to denote a proper averaging or weighting of fluid flow at the interface or along the connection between two blocks or nodes i and j. The convention for the

signs of flow terms is that flow from node j into node i is defined as "+" (positive) in calculating the flow terms. The mass sink/source in Equation (11) at node i, Q_i^k, is defined as the mass exchange rate per time. It is normally used to treat boundary conditions, such as production and injection through wells.

Note that Equation (17) presents a precise form of the balance equation for each mass component in a discrete form. It states that the rate of change in mass accumulation (plus degradation/generation, if existing) at a node over a time step is exactly balanced by inflow/outflow of mass and also by sink/source terms, when existing for the node. As long as all flow terms have flow from node i to node j equal to and opposite to that of node j to node i for fluids, no mass will be lost or created in the formulation during the solution. Therefore, the discretization in (17) is conservative.

Numerical Solution Scheme: There are a number of numerical solution techniques that have been developed in the literature over the past few decades to solve the nonlinear, discrete equations of reservoir simulation. When handling multiphase flow and transport in a multiphase flow system, the predominant approach is to use a fully implicit scheme. This is due to the extremely high nonlinearity inherent in those discrete equations and the many numerical schemes with different level of explicitness that fail to converge in practice. In this section, we discuss a general procedure to solve the discrete nonlinear Equation (17) fully implicitly, using a Newton iteration method. Let us write the discrete non-linear Equation (17) in a residual form as

$$R_i^{k,n+1} = \left\{ M_i^{k,n+1} + G_i^{k,n+1} \Delta t - M_i^{k,n} \right\} \frac{V_i}{\Delta t} - \sum_{j \in \eta_i} flow_{ij}^{k,n+1} - Q_i^{k,n+1} = 0 \qquad (21)$$

(k = 1, 2, and 3; i = 1, 2, 3, ..., N).

Equation (21) defines a set of $(3 \times N)$ coupled nonlinear equations that need to be solved for every balance equation of mass components, respectively. In general, 3 primary variables per node are needed to use the Newton iteration for the associated 3 equations per node. The primary variables selected are oil pressure and two fluid saturations. The rest of the dependent variables, such as relative permeability, capillary pressures, viscosity and densities, and permeability, flow resistance factor, threshold pressure gradient, etc., as well as nonselected pressures and saturations are treated as secondary variables.

In terms of the primary variables, the residual equation (21) at a node i is regarded as a function of the primary variables at not only node i, but also at all its direct neighboring nodes j. The Newton iteration scheme gives rise to

$$\sum_m \frac{\partial R_i^{k,n+1}(x_{m,l})}{\partial x_m} (\delta x_{m,l+1}) = -R_i^{k,n+1}(x_{m,l}) \qquad (22)$$

where x_m is the primary variable m with m = 1, 2, and 3, respectively, at node i and all its direct neighbors; l is the iteration level; and i = 1, 2, 3, ..., N. The primary variables in Equation (17) need to be updated after each iteration:

$$x_{m,l+1} = x_{m,l} + \delta x_{m,l+1} \qquad (23)$$

The Newton iteration process continues until the residuals $R_n^{k,n+1}$ or changes in the primary variables $\delta x_{m,l+1}$ over an iteration are reduced below preset convergence tolerances.

Numerical methods are used to construct the Jacobian matrix for Equation (22), as outlined in Forsyth et al. (1995). At each Newton iteration, Equation (22) represents a system of $(3 \times N)$ linearized algebraic equations with sparse matrices, which are solved by a linear equation solver.

Treatment of Initial and Boundary Conditions: A set of initial conditions is required to start a transient simulation, i.e., a complete set of primary variables need to be specified for every gridblock or node. A commonly used procedure for specifying initial conditions is the restart option, in which a complete set of initial conditions or primary unknowns is generated in a previous simulation with proper boundary conditions described.

Because of more physical and chemical constraints, boundary conditions for a multiphase flow and transport problem are generally much more difficult to handle than for a single-phase situation. When using a block-centered grid, first-type or Dirichlet boundary conditions, can be effectively treated with the "inactive cell" or "big-volume" method, as normally used in the TOUGH2 code (Pruess et al. 1999). In this method, a constant pressure/saturation node is specified as an inactive cell or with a huge volume, while keeping all the other geometric properties of the mesh unchanged. Certain flux-type boundary conditions and more general types of flux- or mixed-boundaries, such as multilayered wells, are part of the solution, and general procedures of handling such boundary conditions are discussed in (Wu et al. 1996; Wu 2000).

Summary

This paper presents our new experimental results on behavior and characteristics of particle gel transport through porous media. Based on our current and previous experimental studies, we propose a conceptual model to investigate PG dynamics as involved in oil production form waterflooding reservoirs. The model is able to predict and evaluate the effects of PG as a controlling agent for improving oil production by waterflooding and the application of the model will be reported in a following study.

References

1. Al-Anaza, and Sharma, M., "Use of a pH Sensitive Polymer for Conformance Control," paper SPE 73782, presented at 2002 International Symposium and Exhibition on Formation Damage Control, Lafayette, Louisiana, 20-21 February, 2002

2. Bai, B., "Development and Application of In-depth Fluid Diversion Technology," RIPED final research report, 2001.

3. Bai, B., et al., "Preformed Particle Gel for Conformance Control: Factors Affecting its Properties and Applications", paper SPE 89389 presented at SPE/DOE at the 2004 SPE/DOE 14th Symposium on IOR held in Tulsa, OK, U.S.A., April 17–21, 2004.

4. Bai, B., et al., "Conformance Control by Preformed Particle Gel: Factors Affecting its Properties and Applications," *SPE Reservoir Evaluation and Engineering*, pp.415-421, Aug 2007.

5. Bai, B., et al., "Preformed Particle Gel for Conformance Control: Transport Mechanism through Porous Media," *SPE Reservoir Evaluation and Engineering*, pp.176-184, April 2007.

6. Bai, et al., "Case Study on Preformed Particle Gel for In-Depth Fluid Diversion, paper SPE 113997, presented at SPE/DOE at the 2008 SPE/DOE 16th Symposium on IOR held in Tulsa, OK, U.S.A., April 20–23, 2008.

7. Chauveteau, G., Omari, A., Tabary, R., Renard, M., and Veerapen, J.: "New Size-Controlled Microgels for Oil Production, paper SPE 64988 presented at the 2001 SPE International Symposium on Oilfield Chemistry, Houston, Feb 13-16, 2001.

8. Chauveteau, G., Tanary, R., Le Bon, C., Renard, M., Feng, Y. and Omari, A., "In-depth Permeability Control by Adsorption of Soft Size-Controlled Microgels," paper SPE 82228, presented at the 2003 SPE European Formation Damage Conference, The Hague, The Netherlands, May 13-14, 2003.

9. Cheung, S., Ng, R., Frampton, H., Chang, K.T., and Morgan, J., "A Swelling Polymer for In-depth Profile Modification: Update on Field Applications," presented at SPE Applied Technology Workshop of "Chemical Methods of Reducing Water Production," San Antonia, Texas, USA, March 4-6, 2007.

10. Coste, J.-P., Liu, Y., Bai, B., Li, Y., Shen, P., Wang, Z., and Zhu, G., "In-Depth Fluid Diversion by Pre-Gelled Particles. Laboratory Study and Pilot Testing," paper SPE 59362, presented at 2000 SPE/DOE Improved Oil Recovery Symposium, Tulsa, Oklahoma, 3-5 April, 2000.

11. Forsyth, P. A., Wu, Y. S. and Pruess, K., "Robust numerical methods for saturated-unsaturated flow with dry initial conditions in heterogeneous media," *Advance in Water Resources,* 18, pp.25-38, 1995.

12. Frampton, et al., "Development of a Novel Waterflood Conformance Control System", paper SPE 89391, presented at the 2004 SPE/DOE 14th Symposium on IOR held in Tulsa, OK, U.S.A., April 17–21, 2004.

13. Huh, C., Choi, S.K., and Sharma, M.M., "A Rheological Model for pH-Sensitive Ionic Polymer Solutions for Optimal Mobility-Control Applications," paper SPE 96914 presented at 2005 Annual Technical Conference and Exhibition, 9-12 October, Dallas, Texas, 2005.

14. Li, Y., Liu, Y., Bai, B., "Water Control Using Swollen Particle Gels," *Petroleum Drilling and Production Technology*, Vol 21(3), 1999.

15. Liu, Y. et al., "Application and Development of Chemical-Based Conformance Control Treatments in China Oil Fields," Paper SPE 99641, presented at the 2006 SPE/DOE Symposium on Improved Oil Recovery, Tulsa, Oklahoma, USA, April 22-26.

16. Jain, R., McCool, C.S., Green, D.W., Willhite, G.P., Michnick, M.J., "Reaction Kinetics of the Uptake of Chromium (III) Acetate by Polyacrylamide," *SPE Journal*, vol 10(3), pp. 247-255, Sept. 2005.

17. Pritchett, J., Frampton, H., Brinkman, J., Cheung, S. Morgan, J., Chang, K.T., Williams, D., Goodgame, J., "Field Application of a New In-Depth Waterflood Conformance Improvement Tool," paper SPE 84897, presented at 2003 International Improved Oil Recovery Conference in Asia Pacific, 20-21 October, Kuala Lumpur, Malaysia, 2003.

18. Pruess, K., Oldenburg, C. and Moridis, G., *TOUGH2 User's Guide, Version 2.0,* Report LBNL-43134, Berkeley, California: Lawrence Berkeley National Laboratory, 1999.

19. Pruess, K., *TOUGH2 - A General-Purpose Numerical Simulator for Multiphase Fluid and Heat Flow*, Report LBL-29400, Lawrence Berkeley National Laboratory, Berkeley, California, 1991.

20. Rousseau, D., Chauveteau, G., Renard, M., Tabary, R., Zaitoun, A., Mallo, P., Braun, O. and Omari, A., "Rheology and Transport in Porous Media of New Water Shutoff/Conformance Control Microgels," paper SPE 93254, presented at the 2005 SPE Int. Symp. On Oilfield Chemistry, Houston, TX, USA, Feb 2-4, 2005.

21. Seright, R.S., "Conformance Improvement Using Gels," Annual Technical Progress Report (U.S. DOE Report DOE/BC/15316-6), U.S. DOE Contract DE-FC26-01BC15316, 72, Sept. 2004.

22. Sydansk, R.D. et al., "Characterization of Partially Formed Polymer Gels for Application to Fractured Production Wells for Water-Shutoff Purposes," *SPE Production & Facilities*, Vol 20 (3), pp.240-249, Aug, 2005.

23. Sydansk, R.D. et al., "Polymer Gels Formulated With a Combination of High- and Low-Molecular-Weight Polymers Provide Improved Performance for Water-Shutoff Treatments of Fractured Production Wells," *SPE Production & Facilities,* Vol.19 (4), pp.229-236, 2004.

24. Wu, Y.S., "A virtual node method for handling wellbore boundary conditions in modeling multiphase flow in porous and fractured media," *Water Resources Research*, 36 (3), pp.807-814, 2000.

25. Wu, Y.S., Forsyth, P. A. and Jiang, H.: "A consistent approach for applying numerical boundary conditions for subsurface flow," *Journal of Contaminant Hydrology*, Vol. 23, pp.157-185, 1996

26. Wu, Y. S., Pruess, K., and Witherspoon, P.A., "Flow and Displacement of Bingham Non-Newtonian Fluids in Porous Media," *SPE Reservoir Engineering*, pp.369-376, Aug. 1992.

27. Zaitoun, A., Tabary, R., Rousseau, D., Pichery, T., Nouyoux, S., Mallo, P., and Braun, O., "Using Microgels to Shutoff Water in Gas Storage Wells," paper SPE106042 presented at 2007 SPE International Symposium on Oilfield Chemistry, Houston, TX, USA, 28 Feb - 2 March, 2007.